SLAC-PUB-2949
July 1982
(T/E)

MEASUREMENT OF ELASTIC ELECTRON-NEUTRON CROSS SECTIONS UP TO $Q^2 = 10$ (GeV/c)^2*

S. Rock, R. G. Arnold, P. Bosted, B. T. Chertok,† B. A. Mecking,‡ I. Schmidt,§ Z. M. Szalata, R. C. York,** and R. Zdarko

Department of Physics
The American University, Washington, D.C. 20016
and
Stanford Linear Accelerator Center
Stanford University, Stanford, California 94305

ABSTRACT

We measured the elastic electron-neutron cross sections at four-momentum transfers squared (Q^2) of 2.5, 4.0, 6.0, 8.0 and 10.0 (GeV/c)^2 using a deuterium target and detecting the scattered electrons at 10°. The ratio of neutron to proton elastic cross sections decreases with Q^2. At high Q^2 this trend is inconsistent with the dipole law, form factor scaling, and many vector dominance models, although it is consistant with some parton models.

(Submitted to Physical Review Letters)

---

*Work supported by the Department of Energy, contract DE-AC03-76SF00515.

Determining the structure of the nucleons is one of the fundamental problems of physics. A wide variety of empirical and theoretical models ranging from form factor scaling[1] and vector dominance[2] to quark-parton models[3] and perturbative QCD[4] have been used to explain the elastic cross sections (σ_p, σ_n). Most of the current models agree with existing data but diverge from each other in the previously unexplored region of high four-momentum transfer squared (Q^2). While σ_p has been measured[5] up to $Q^2 = 33$ $(GeV/c)^2$, σ_n had been reliably measured[6] only to $Q^2 = 4$ $(GeV/c)^2$. Here we report measurements of σ_n out to $Q^2 = 10.0$ $(GeV/c)^2$.

The cross section for elastic electron-nucleon scattering can be written as:

$$d\sigma/d\Omega = \sigma_M [A(Q^2) + B(Q^2) \tan^2(\tfrac{1}{2}\theta)] \qquad (1)$$

where σ_M is the Mott cross section, $A = (G^2_E + \tau G^2_M)/(1 + \tau)$, and $B = 2\tau G^2_M$. The electric form factor G_E and the magnetic form factor G_M are functions of Q^2 only, $\tau = Q^2/4m^2$, and $Q^2 > 0$ in the spacelike region. Since the contribution from G_M dominates that of G_E by a factor of τ, and G_E is thought to be small for the neutron, our measurements at large Q^2 are mostly sensitive to G_M.

The experiment was done in End Station A at SLAC. We detected electrons scattered from 30 cm long hydrogen or deuterium targets into the 20 GeV/c spectrometer[7] set at 10°. The momentum (E') and polar angle (θ) of the electrons were measured with five planes of MWPCs. Electrons were identified in a total-absorbtion shower counter. We determined the spectrometer acceptance with slits and by collecting over

a million events in the deep inelastic region where the spectrum is flat.

For each incident energy we measured the electron-deuteron and electron-proton cross sections $\sigma(\Omega, E')$ over the entire quasielastic region and well into the inelastic region in eight overlapping steps in spectrometer momentum. The cross sections measured in the overlapped regions were in excellent agreement. High statistics were necessary to determine the precise shapes of the spectra so that we could separate them into elastic and inelastic components. For example at $Q^2 = 6$ $(GeV/c)^2$ we collected approximately 6×10^4 e-d events. About 60% of them were in the quasielastic peak region, yielding ~3% statistical accuracy in each of 40 bins in E'. The experimental cross sections were radiatively corrected using an iterative method based on the work of Mo and Tsai[8] to get the true cross sections. The cross section at $Q^2 = 6.0$ $(GeV/c)^2$ is shown as the points in Fig. 1. Notice that the quasielastic peak at $E' = 12.55$ GeV is partly obscured by the inelastic cross section.

As a calibration we compared the elastic e-p cross sections extracted from our hydrogen target data with previous data at all five values of Q^2. Our results agree with a fit to the world data[9] to within the statistical errors of a few percent.

In the impulse approximation the scattering from deuterium is the sum of scattering from the individual moving nucleons. At our elastic scattering kinematics this Fermi motion causes a momentum smear of about ±1.5 percent FWHM which means that the quasielastic and long tail of the

smeared inelastic spectrum overlap at high Q^2. To extract the quasielastic neutron cross section from the deuteron data, the quasielastic proton and smeared inelastic proton and neutron cross sections must be subtracted. The quasielastic neutron cross section is proportional to the smeared elastic proton cross section, $(\sigma_{p,el})_{sm}$. The smeared inelastic neutron cross section was assumed to be proportional to the smeared inelastic proton cross section, $(\sigma_{p,in})_{sm}$, over our limited range of E'. The smeared proton cross sections were obtained from our hydrogen data supplemented at high inelasticity by the extensive data taken by other groups at SLAC.[10] The Fermi momentum (p_f) distribution was obtained from models[11] of the deuteron wave function.

Two independent methods were used to obtain these smeared proton cross sections. In the first method a Monte Carlo program generated kinematic quantities for elastic and inelastic electrons scattered from moving nucleons. The events were radiated and they were weighted by the deuterium wave function and the cross section. The events were reduced to cross sections by the same procedure as for the real data and then compared with the experimental deuterium cross sections. In the second method we used analytical expressions derived from the work of McGee[12] to calculate the quasielastic and smeared inelastic cross sections. The latter were treated as the sum of narrow elastic-like peaks. These smeared cross sections were compared with the radiatively corrected deuterium cross sections.

In both methods the measured deuterium spectrum was represented by the expression:

$$\sigma(\Omega, E') = R_{el} \cdot (\sigma_{p,el})_{sm} + R_{in} \cdot (\sigma_{p,in})_{sm} \quad .$$

The proportionality constants $R = \sigma_d/\sigma_p = (\sigma_n + \sigma_p)/\sigma_p$ are determined by a least squares fit. In Fig. 1 the radiatively corrected deuterium spectrum, the quasielastic and smeared inelastic proton spectra, and the fit are shown for $Q^2 = 6.0$ (GeV/c)^2.

The good fits at each value of Q^2 support the validity of the assumptions going into the analysis. We studied extensively the sensitivity of the results to various inputs to the analysis and found the largest variations to come from the use of a variety of deuteron wave functions with different high momentum components for $p_f > 0.25$ GeV/c, and from the two different methods of analysis. The systematic errors are larger than the statistical ones. The errors we present enclose the results for both methods with three different realistic deuteron wave function models:[11] the Paris potential, the Bonn potential, and the Reid Soft Core modified by recent[13] Saclay Data.

Table I lists the ratio $\sigma_n/\sigma_p = R_{el} - 1$, the values of the neutron cross section obtained by using our elastic e-p results for σ_p, and G_{Mn} extracted from Eq. (1) assuming $G_{En} = 0$. The ratio σ_n/σ_p is shown in Fig. 2 as a function of Q^2 along with some results from a previous experiment (Albrecht, Ref. 6). Notice that our results are consistent with the other results, but are a little lower. We show the predictions from two commonly used empirical relationships: the dipole law $G_{Mn} = \mu_n/(1 + Q^2/0.71)^2$ with σ_p from our data (dash-dot), and form factor scaling $G_{Mn} = \mu_n G_{Mp}/\mu_p$ (dotted), both with $G_{En} = 0$. The dashed curve is the model of Höhler et al.[2] which is typical of other VDM calculations.

The new high Q^2 data fall well below these curves. The solid curve is the VDM prediction of Blatnik and Zovko[2] which incorporates the asymptotic limits discussed below.

The quark dimensional scaling laws[14] predict that at large Q^2 the spin averaged hadronic elastic form factor $\sqrt{A(Q^2)}$ has a power law dependence $(1/Q^2)^{n-1}$ where n is the number of elementary quark constituents. In Fig. 3 we plot the experimental values $(Q^2)^{n-1}[\sigma/\sigma_M]^{1/2}$ (= $(Q^2)^{n-1}\sqrt{A(Q^2)}$ at small angles) versus Q^2 for the pion, the nucleons, and several light neuclei.[15]. Within the errors our new neutron form factor data scale.

Explicit calculations[14] for the nucleon using a model with 3 spin 1/2 quarks show that at large Q^2, $F_1(Q^2) = C_1/(Q^2)^2$ and $F_2(Q^2) = C_2/(Q^2)^3$ where $F_1 = (G_E + \tau G_M)/(1-\tau)$ and $F_2 = (G_E - G_M)/k(\tau - 1)$ are the Dirac and Pauli form factors, and k is the anomalous magnetic moment. The C_1 and C_2 depend on the quark wave function of the nucleons and in particular on the average charge of the leading quark near $x = 1$. If the nucleon wave function is spacially symmetric such that $F_{1n} \to 0$ then $\sigma_n/\sigma_p \to 1/Q^2$ at large Q^2. Alternatively, if the leading quark has the same isospin[15] (helicity[16]) as the nucleon it follows that $\sigma_n/\sigma_p \to 1/4$ (1/9). Our results show σ_n/σ_p falling with increasing Q^2 above $Q^2 = 6$ $(GeV/c)^2$ in a way which is consistent with all three predictions.

There are assymptotic perturbative QCD calculations[4] in which the power law Q^2 dependence of the form factors given by the dimensional scaling laws (modulo logarithmic corrections) arises from the hard scattering subprocesses involving all the valence quarks. The form

factors also depend on the quark wave functions. The calculation of Brodsky and Lepage shows G_{Mn}/G_{Mp} to be particularly sensitive to the wave functions, and for a wide range of possible wave functions they predict $\sigma_n/\sigma_p = (G_{Mn}/G_{Mp})^2 > 1$. This is inconsistent with our results and the trend with increasing Q^2 is in the opposite direction. This could indicate that these asymptotic predictions are not applicable at our Q^2, or that there are some fundamental problems with perturbative QCD. In any case these results will severely restrict models for the nucleon wave functions.

We acknowledge Dave Sherden for his help with our new computer and the Spectrometer Facilities Group for their support. This work was supported by the Department of Energy under contract DE-AC03-76SF00515 and National Science Foundation grants PHY78-09378 and PHY81-08484.

REFERENCES

[†]Deceased 1981.

[‡]On leave from Universitat Bonn, West Germany.

[§]Now at: University of Santiago, Chile.

**Now at: University of Virginia, Charlottesville, VA.

[1]T. Narita, Progress in Theoretical Physics 42, 1336 (1969); A. L. Licht and A. Pagnamenta, Phys. Rev. D 4, 2810 (1971).

[2]F. Iachello et al., Phys. Lett. 43B, 191 (1973); S. Blatnik and N Zovko, Acta Physica Austriaca 39, 62 (1974); F. Felst, DESY preprint 73/56, unpublished; G. Höhler et al., Nucl. Phys. B114, 505 (1976).

[3]S. D. Drell and T. M. Yan, Phys. Rev. Lett. 24, 181 (1970); S. J. Brodsky and B. Chertok, Phys. Rev. D 14, 3003 (1976);

[4]S. J.Brodsky and G. P. Lepage, Physica Scripta 23, 945 (1981); G. P. Lepage and S. J. Brodsky, Phys. Rev. D 22, 2157 (1980).

[5]P. N. Kirk et al., Phys. Rev. D 8, 63 (1973); S. Stein et al., Phys. Rev. D 12, 1884 (1975); W. B. Atwood, PhD Thesis, SLAC Report No. 185 (1975), SLAC, Stanford, CA.

[6]W. Bartel et al., Nuc. Phys. B58, 429 (1973); K. Hanson et al., Phys. Rev. D 8, 753 (1973); R. J. Budnitz et al., Phys. Rev. 173, 1357 (1968); W. Albrecht et al., Phys. Lett. 26B, 642 (1968).

[7]L. W. Mo, SLAC-TN-65-40 (1965), SLAC, Stanford, CA; S. Stein et al., Phys. Rev. D 12, 1884 (1975).

[8]L. W. Mo and Y. S. Tsai, Rev. Mod. Phys. 41, 205 (1969); Y. S. Tsai, SLAC-PUB-848 (1971), SLAC, Stanford CA.

[9]We use the fit dipole (Γ_ρ = 112 MeV) from Iachello et al., Ref. 2.

[10]A. Bodek et al., Phys. Rev. D 20, 1471 (1979); M. D. Mestayer, PhD Thesis, SLAC Report No. 214 (1978), SLAC, Stanford CA; J. S. Poucher et al., SLAC-PUB-1309 (1973), SLAC, Stanford CA.

[11]R. V. Reid, Jr., Ann. Phys. (N.Y.) 50, 411 (1968); The Bonn potential: K. Holinde and R. Machleidt, Nucl. Phys. A256, 479 (1976); The Paris potential: M. Lacombe et al., Phys. Rev. D 12, 1495 (1975); C21, 861 (1980).

[12]W. Bartel et al., Nucl. Phys. B58, 429 (1973); I. J. McGee, Phys. Rev. 161, 1640 (1967).

[13]M. Bernheim et al., Nucl. Phys. A365, 349 (1981).

[14]S. J. Brodsky and G. Farrar, Phys. Rev. D 11, 1309 (1975).

[15]S. J. Brodsky and B. Chertok, Phys. Rev. D 14, 3003 (1976); and for the He data: R. G. Arnold et al., Phys. Rev. Lett. 40 1429 (1978).

[16]G. Farrar and D. Jackson, Phys. Rev. Lett. 35, 1416 (1975).

Table I. The ratios of elastic electron-neutron to elastic electron-proton cross sections, the values of the neutron cross section, and G_{Mn} extracted from our data using Eq. 1 assuming $G_{En} = 0$. The errors include statistical and systematic effects.

Q^2 $(GeV/c)^2$	σ_n/σ_p	σ_n (nb)	G_{Mn}
2.5	0.37 ± 0.03	2.9 ± 0.2	0.092 ± 0.004
4.0	0.37 ± 0.03	0.42 ± 0.03	0.041 ± 0.002
6.0	0.38 ± 0.04	0.070 ± 0.007	0.0195 ± 0.0010
8.0	0.25 ± 0.08	0.012 ± 0.004	0.0090 ± 0.0015
10.0	0.21 ± 0.10	0.0031 ± 0.0015	0.0053 ± 0.0013

FIGURE CAPTIONS

Fig. 1. The cross sections for e-d scattering at incident energy E = 15.742 GeV versus scattered electron energy E′ at 10°. The dashed (dotted) curve is the smeared elastic (inelastic) e-p cross section obtained with Method II and the Paris potential (Ref. 11). The solid curve is the result of a linear least squares fit of the other two curves to the e-d cross section as described in the text. All cross sections are radiatively corrected.

Fig. 2. The ratio σ_n/σ_p as a function of Q^2. Previous data from Albrecht et al. (Ref. 6) has been extrapolated to 10°. The dashed and solid curves are the VDM models of Höhler et al., and Blatnik and Zovko (Ref. 2) respectively. The dotted curve is form factor scaling: $G_{Mn}/\mu_n = G_{Mp}/\mu_p = G_{Ep}$ and $G_{En} = 0$. The dash-dot curve is the dipole law for G_{Mn} with $G_{En} = 0$ and σ_p from our experimental results.

Fig. 3. Quark dimensional scaling of the elastic form factors of the pion, nucleons and three light nuclei. The power n is the number of elementary quark constituents.

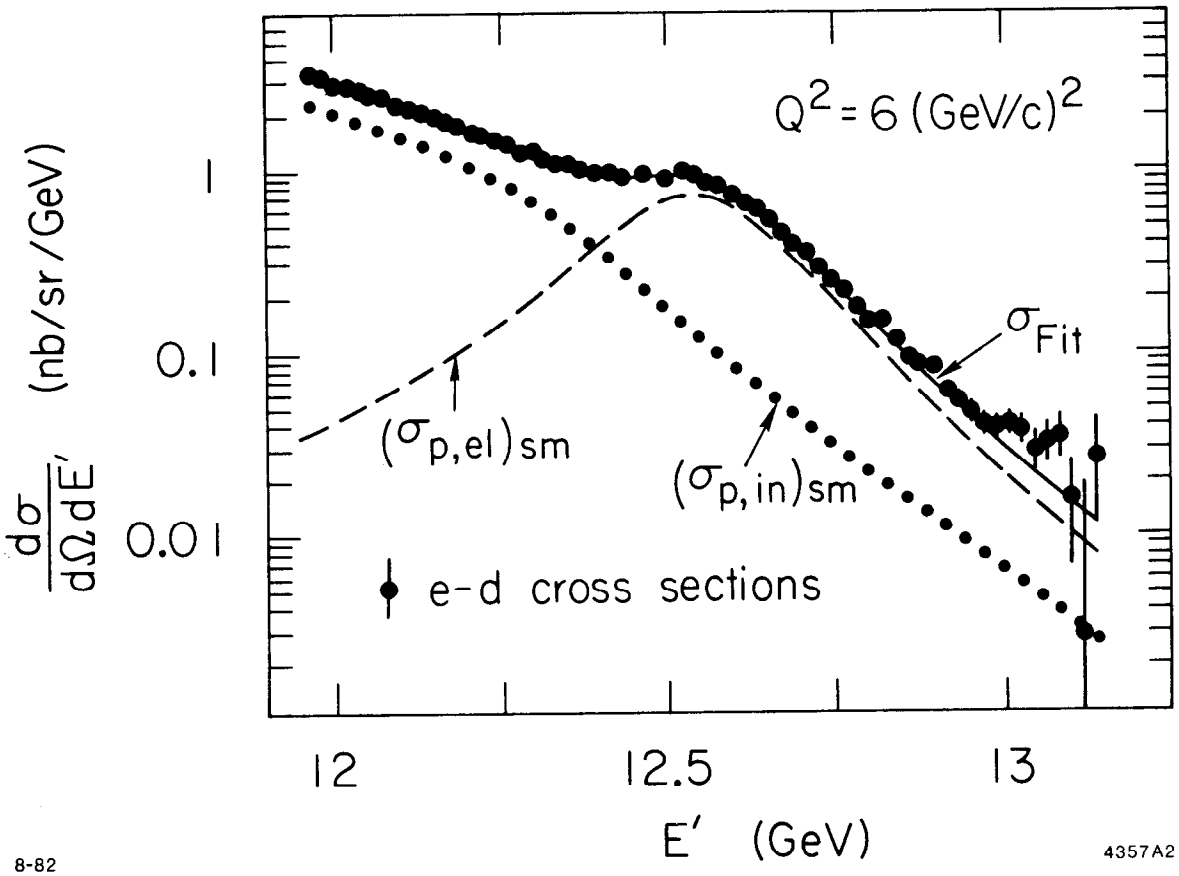
$Q^2 = 6\ (GeV/c)^2$
σ_{Fit}
$(\sigma_{p,el})_{sm}$
$(\sigma_{p,in})_{sm}$
e-d cross sections
$\frac{d\sigma}{d\Omega dE'}$ (nb/sr/GeV)
1
0.1
0.01
12
12.5
13
E′ (GeV)
8-82
4357A2

Fig. 1

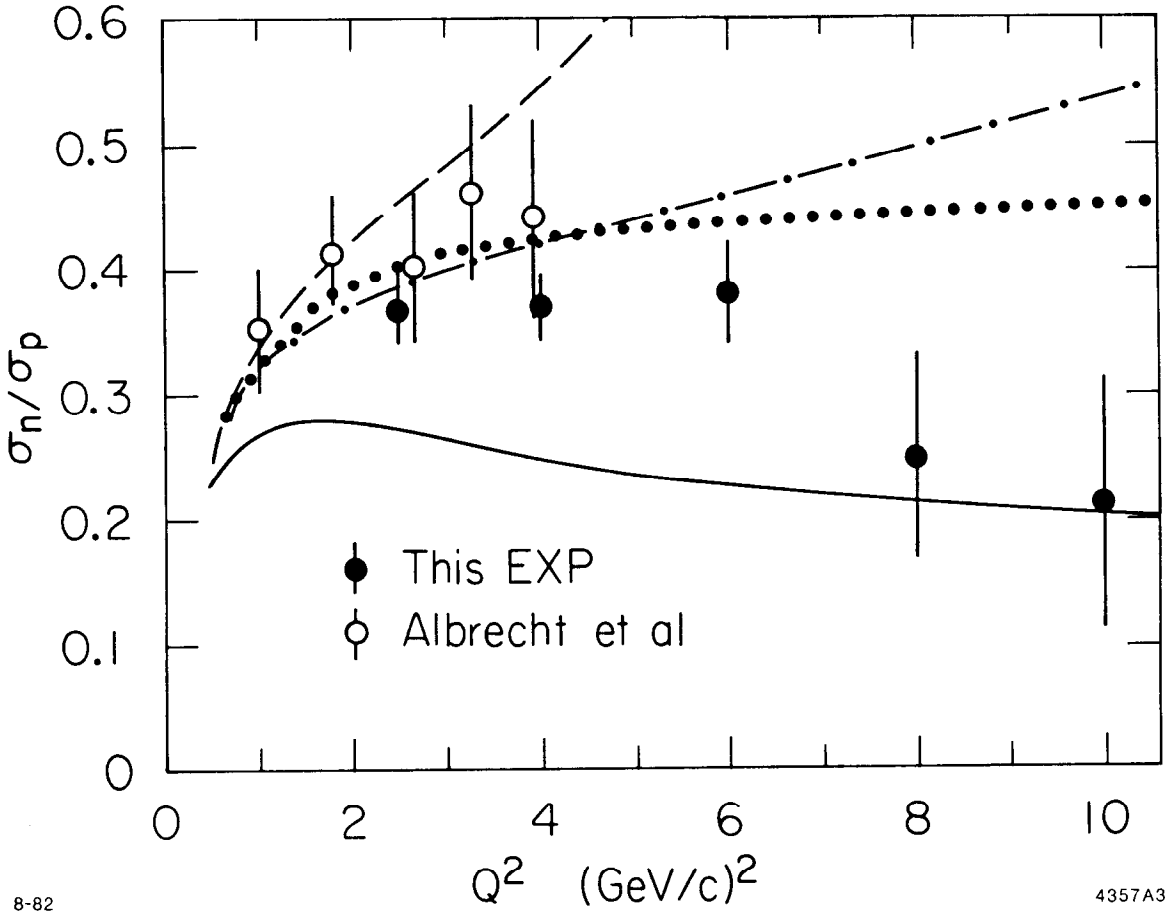
0.6
0.5
0.4
0.3
0.2
0.1
0
σ_n/σ_p
This EXP
Albrecht et al
0
2
4
6
8
10
Q^2 (GeV/c)^2
8-82
4357A3

Fig. 2

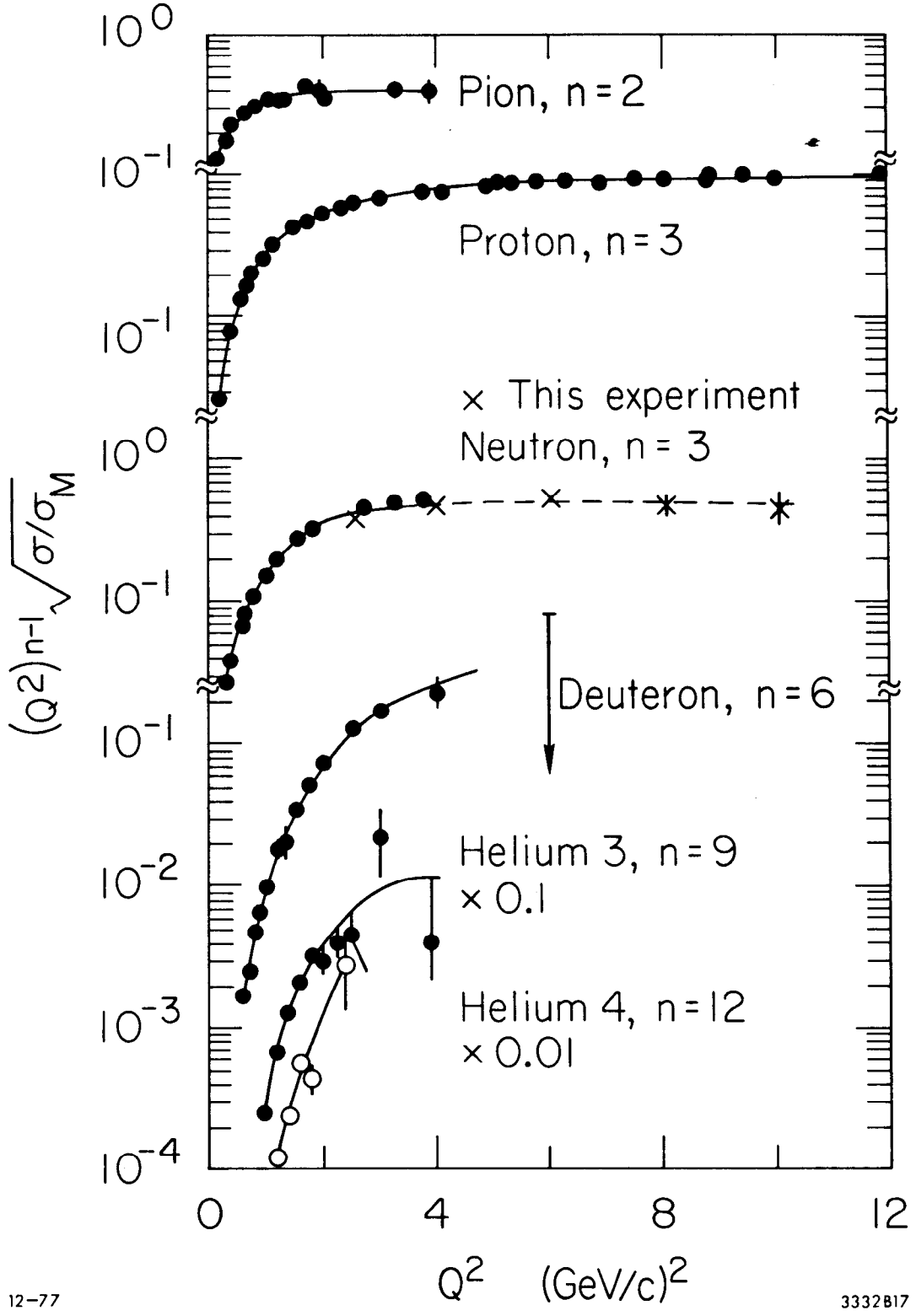
Pion, n = 2
Proton, n = 3
× This experiment
Neutron, n = 3
Deuteron, n = 6
Helium 3, n = 9
× 0.1
Helium 4, n = 12
× 0.01
$(Q^2)^{n-1}\sqrt{\sigma/\sigma_M}$
Q^2 $(GeV/c)^2$
10^0
10^{-1}
10^{-2}
10^{-3}
10^{-4}
0
4
8
12
12-77
3332B17

Fig. 3